Available online at www.sciencedirect.com
ScienceDirect
Journal of Molecular Structure 873 (2008) 121–129
Journal of MOLECULAR STRUCTURE
www.elsevier.com/locate/molstruc

Modeling of ZnS quantum dots synthesis by DFT techniques

Alvaro A.A. de Queiroz *, Mayler Martins, Demétrio A.W. Soares, Écio J. França

Departamento de Física e Química/Instituto de Ciências Exatas, Universidade Federal de Itajubá (UNIFEI), Itajubá – MG, Brazil

Received 7 August 2006; received in revised form 6 March 2007; accepted 6 March 2007
Available online 14 March 2007

Abstract

Zinc sulfide (ZnS) and doped zinc sulfide (ZnS:Cu) were prepared by the polyol process using polyethylene glycol (PEG) as the ceramic precursor. Thiourea (TU) was employed for in situ generation of ZnS ceramic powder. X-ray diffraction (XRD), scanning electron microcopy (SEM), absorption and photoluminescence (PL) spectra were used to characterize the luminescent ceramic. The structure, surface morphology, chemical composition and optical properties of the inorganic phosphors were investigated as function of copper doping. Both XRD and SEM indicated that the particles present good crystalline state, whose crystalline grain sizes were in the range around 50–60 μm. The reactivity of both, PEG:Zn^{2+} and PEG:Zn^{2+}:TU was interpreted by means of the potential energy surfaces determined by density functional theory (DFT) computations. The analysis of the local ionization surfaces and frontier orbitals was used to study the reactivity of the PEG:Zn^{2+}:TU as ZnS nanocrystals precursor.
© 2007 Elsevier B.V. All rights reserved.

Keywords: Quantum dots; Luminescent materials; DFT computations; ZnS, Local density approximation

1. Introduction

Semiconductor nanocrystals in which mobile electrons reside in a specific spatial region, such as a thin quantum well formed by heterojunction layers on the order of 100 Å in thickness, more commonly known as quantum dots, were initially studied over the past of three decades because of their potential in assisting the development of new electronics and optical devices [1].

Semiconductor quantum dots based on luminescent properties of group II and VI elements (e.g. ZnS, CdS, CdSe) have attracted special interests of scientists and engineers due to their fascinating optical and electronic properties [2–19]. It is may be emphasized that quantum dots (QDs) contain only a few hundred atoms and emit only one wavelength of light when they are excited. The color emitted is determined by the size of the quantum dots.

Recently, research has stimulated considerable interest in developing the ZnS QDs as fluorescent probes for biomedical applications to help diagnose disease or discover new drugs through their florescent tagging capabilities [20–26]. Fluorescence is a luminescence phenomena that occurs in luminescent materials where after absorbing light of a particular wavelength occurs re-emission of a quantum of light with an energy corresponding to the energy difference between the excited state and the ground state [27]. The energy-level diagram shown in Scheme 1 illustrates the luminescence mechanism of ZnS nanoparticles. The valence band largely consists of hybridized s–p orbitals from sulfur and zinc atoms, while the conduction band is mainly due to the s–p antibond states of ZnS [28]. The sulfur vacancies in ZnS exert a potential, which can attract and trap electrons and generate delocalized donor sites with an energy level just below the conduction band. The emission occurs when a trapped electron recombines with a hole in the valence band or in some acceptor level [29].

It is well known that the luminescence characteristics of impurity-activated ZnS are size-dependent of the nanocrystals as well as the chemical composition of the doping agent [30,31]. In this sense, when zinc sulfide is activated with copper (ZnS:Cu), a green light emission ($\lambda = 520$ nm) is

* Corresponding author. Tel.: +55 35 3629 1435; fax: +55 35 3629 1440.
E-mail address: alencar@unifei.edu.br (A.A.A. de Queiroz).

0022-2860/$ - see front matter © 2007 Elsevier B.V. All rights reserved.
doi:10.1016/j.molstruc.2007.03.013

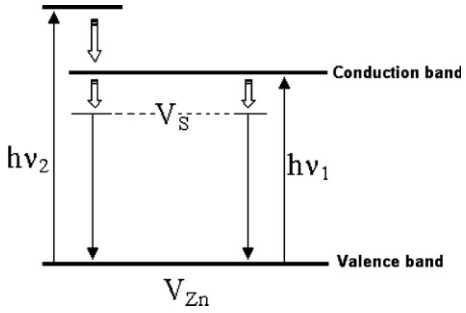

Scheme 1. Luminescence mechanism of ZnS nanoparticles V_{Zn} represents the acceptor level at zinc and V_S the sulfur vacancy donor level.

induced that could be convenient to use the ZnS:Cu nanocrystals in mammography [32].

Many methods have been developed to produce ZnS nanocrystals with adequate optoelectronic properties such as spray pyrolysis [33], molecular chemical vapor deposition (MOCVD) [34], plasma chemical sputtering [35], solid-state methodologies [36], lamellar precursors [37] and chemical bath deposition (CBD) [38]. However, the major disadvantages in the preparation of ZnS:Cu nanocrystals by these methods are the poor distribution of the nanoparticle size, the aggregation of the nanocrystals and the heat treatment or high pressure in the synthesis conditions, which makes the preparing procedure more complex and difficult.

A valuable and promising alternative route to produce ZnS:Cu nanocrystals may be the use of polymeric precursors and have attracted the interests of researchers to inhibit the formation of hard agglomerates and a better compositional homogeneity of the ZnS powder [39–41].

In spite of the large number of investigations there are few studies on the synthesis of ZnS phosphors using the poly(ethylene glycol) (PEG) system as reaction medium in order to stabilize the nanocrystals of the luminescent material in the colloidal form and, as far the authors are aware, no molecular modeling about the stability of the PEG:Zn charge–transfer complexes were reported still the moment. The physical isolation of individual nanocrystals is essential for quantum confinement effects. In this sense, the OH groups of PEG may be favorable to the nucleation sites for preparing nanocrystals of ZnS playing an important role in the luminosity of the resultant nanophosphor.

In this work the experimental conditions for the synthesis of ZnS are studied and the quantum chemistry modeling was performed aiming to obtain a better understanding of the ZnS nanocrystals synthesis at molecular level.

2. Materials and methods

2.1. Preparation of ZnS:Cu

The Cu-doped zinc sulfide (ZnS:Cu) nanocrystals were obtained by precipitation from a homogeneous solution of zinc ($ZnCl_2$, Sigma/Aldrich) and copper ($CuCl_2$; Sigma/Aldrich) with the sulfide ions (S^{2-}) formed by thermal decomposition of thiourea ($(NH_2)_2CS$, Sigma/Aldrich) (TU) as precipitating agent. In a typical preparation, 10 mL of 0.1 M $ZnCl_2$ was mixed with the required quantity of 0.01 M $CuCl_2$ to obtain a desired Cu^{2+} concentration in the reaction medium. The resultant solution was dispersed in polyethylene glycol having a molar mass of 400 g mol^{-1} (PEG 400, Sigma) at molar ratio of 0.3 M and heated at 70 °C. A solution of thiourea (0.5 mol) was slowly added dropwise to the PEG:Zn^{2+} solution. The system was stirred at 1200 rpm followed to reflux between 180 and 200 °C. A colloidal suspension was obtained immediately after thiourea addition. The precipitates was separated by centrifuging and washed several times with distilled water. The ZnS:Cu nanocrystals was thoroughly washed with ethanol to extract the residual impurities and then the finely divided powder was dried under vacuum at 80 °C. The synthesized nanocrystals were annealed in S_2-rich atmosphere at temperature of 850 °C for two hours. The powder thus obtained was found to show bright luminescence under UV excitation, indicating an effective ZnS doping. Undoped ZnS powders were also prepared in the same fashion without addition of copper ions.

2.2. Characterization

The structural characteristics of obtained ZnS:Cu powder were explored by X-ray diffraction method (XRD, Philips PW 1130 X-ray diffractometer system with graphite monochromatized CuK_α irradiation, $\lambda = 1.5418$ Å).

The photoluminescence spectra of the inorganic phosphor were recorded with a Hitachi M-850 fluorescence spectrophotometer equipped with a Xe discharge lamp with 0.8 μs and 20 kW discharge. The discharge frequency is the same as the line frequency (60 Hz) and the average lamp energy output was 10 W. All measurements were carried out at room temperature (27 °C) under ambient atmosphere and the ZnS or ZnS:Cu powder samples were pressed into thin slices so that the measurement parameter of the phosphor was constant.

The form and size of the particles were determined by scanning electron microscopy (SEM, Philips XL 30). The mean size and the standard deviations were estimated from image analysis of ca. 200 particles. The acquisition of SEM images were made using Hlimage++ computer vision systems (1997, Western Vision Software, Salt Lake City, UT, USA). The library, with a considerable number of features, extraction algorithms used for pattern recognition and image analysis as well as acceptance or rejection of samples, was conceived and implemented [42].

Elemental mapping of Cu in the ZnS was carried out using the X-ray photoelectron spectroscopy (ESCA-36, McPherson spectrophotometer).

2.3. Theory

Powerful methods for theoretical and computational investigations of molecular electronic structure have

become available with the advent of more powerful computers during the past century. Recent works have proposed algorithms for generation and visualization of a variety of molecular surfaces in computers to get a three-dimensional representation of the molecular properties under consideration [43].

In recent years, the DFT methods has transformed in a competitive methodology comparative with the semi-empirical models (of computational view point) but much more accurate in the properties determination of the molecular systems, allowing the quantum mechanical treatment of molecular systems with hundreds of atoms.

The density functional theory (DFT) is based on the Hohenberg–Kohn (HK) theorems, which states that the electron density $\rho(\mathbf{r})$, may determine the ground-state energy and other ground-state properties [44]. Moreover, it follows that the true electron density corresponds to the lowest energy. In this sense both, energy and electron density may be optimized by the variational procedures.

The variational problem of minimizing the energy functional was solved by applying the Lagrangian method of undetermined multipliers, which was done by Kohn and Sham (KS) in 1965. The KS orbitals $\phi_i(\mathbf{r})$ and their energies ε_i are obtained by solving the equation [45]

$$\left\{-\frac{\hbar}{2m_e}\nabla_1^2-\frac{e^2}{4\pi\varepsilon_o}\sum_{I=1}^{N}\frac{Z_1}{R_{I1}}+\frac{e^2}{4\pi\varepsilon_o}\int\frac{\rho(\mathbf{r}_2)}{\mathbf{r}_{12}}\,d\mathbf{r}_2+V_{XC}(\mathbf{r}_1)\right\}$$
$$x\phi_i(\mathbf{r}_1)=\varepsilon_i\phi_i(\mathbf{r}_1) \quad (1)$$

where the second term denotes the so-called Hartree term and describe the electron–electron Coulomb repulsion, while the last term V_{XC} is called the exchange correlation potential.

Since the Hartree term and V_{XC} depend on $\rho(\mathbf{r})$, which depends on the ϕ_i, which in turn depend on the effective single-particle potential, the problem of solving the Kohn–Sham equation has to be done in a self-consistent way.

The exchange-correlation potential V_{XC} is defined as a functional derivative of the exchange-correlation energy E_{XC}

$$V_{XC}[\rho]=\frac{\delta E_{XC}[\rho]}{\delta\rho} \quad (2)$$

The major problem with DFT is that the exact functionals for exchange and correlation are not known except for the free electron gas. However, approximations exist which permit the calculation of certain physical quantities quite accurately. The most widely used approximation is the local density approximation (LDA), whereby only the electron density value at a given point in space determines the contribution of this point to the exchange-correlation energy and all non-local effects are neglected. This approximation treats the molecule as containing a homogeneous electron gas in the field of a continuously distributed positive charge. Although this is obviously an unrealistic picture, LDA functionals yield relatively accurate structures.

In this work, we used the DFT–LDA method, with Slater–Dirac exchange [46] and Vosko–Wilk–Nusair [47] correlation (RSVWN1RPA). The Gaussian base used was 6.31G** (with s, p orbital for hydrogen atoms and s, p and d orbitals for the others atoms). After each SCF single point round, was made the energy minimization of the molecular structure using the molecular mechanics force field, MMFF94 [48] method. This methodology allowed us to analyze the charge–transfer interactions in both, PEG:Zn and PEG:Zn:TU structures.

The local ionization potential (LIP) [49,50] mapped on the surface of the total electron density of the molecules is given by

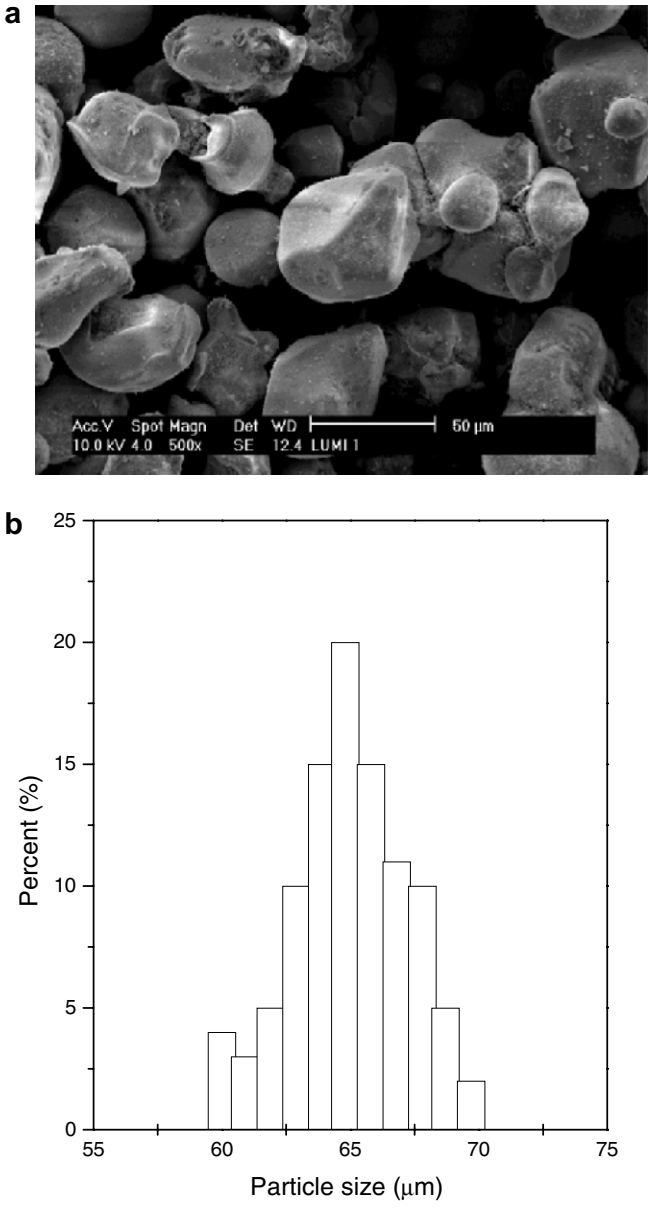

Fig. 1. SEM micrograph of Cu^{2+}-doped ZnS (3 wt%) particles obtained by the polyol process (a) and histogram of the size distribution of these particles (b).

$$I(r) = \sum_{i}^{\text{occupied}} \frac{\rho_i(r)|\varepsilon_i|}{\rho(r)} \quad (3)$$

The summation of Eq. (2) was made over all occupied ρ_i molecular orbital electron densities times and the absolute orbital energies,$|\varepsilon_i|$, divided by the total electron density ρ. The LIP values would be useful to indicate the electrophylic character of the ZnS precursors at molecular level. In this sense, the ionization potential maps may be powerful tools to graphical display the areas where the electrons may be more easily removed. The obtained results of ionization potentials are comparatively to the map of the electrostatic potential [51], but with significant advantages from the view of the computational cost.

3. Results and discussion

Poly(ethylene glycol) (PEG) has attracted considerable attention because of its ability to solvate ions and thus provide metal complexes with many promising applications in chemical synthesis of nanostructured ceramics [52,53].

Fig. 1 shows the SEM micrograph and the particle size distribution of the luminescent ZnS:Cu powder synthesized in this work. The poly(ethylene glycol) 400 appears to induce the nucleation step and this, in turn, favored the monodispersity of particles when more nuclei were formed. As a consequence of PEG controlled nucleation and crystal growth steps, the ZnS:Cu particles possess homogeneous shape with a typical diameter in the range of 60–70 μm and a narrow size distribution (Fig. 1b).

The synthesized ZnS and ZnS:Cu powders characterized by X-ray diffraction showed to be ZnS wurtzite structure with preferred orientation in <100> and <101> directions (Fig. 2a). The measured lattice parameter "*a*" was $3.822 \pm 0{,}002$ Å which is closed to the report value [54,55]. Fig. 2b suggests that the copper ions introduce a strain in the ZnS lattice, substituting the zinc sites and leading to a decrease in the volume of the lattice. ZnS crystallizes as cubic closest-packed array of S^{2-} with Zn^{2+} ions in tetrahedral sites and cell-edge length of 541 pm. The ionic radius of Zn^{2+} (88 pm) is in the near to ionic radius of Cu^{2+} (87 pm). Thus, the fact that the volume of the ZnS lattice decreases with copper doping (Fig. 2b) may be due to the S vacancies since the ion radius of S^{2-} is 174 pm, resulting in the decrease of lattice constants. It is interesting to note that a relatively high Cu doping level in ZnS particles could be achieved (Fig. 2b). Although the solubility product of CuS (2.5×10^{-48}) is far less than that of ZnS (2.2×10^{-22}) which makes it difficult for Cu^{2+} and Zn^{2+} ions to be co-precipitated with S^{2-} ions, the metal complex

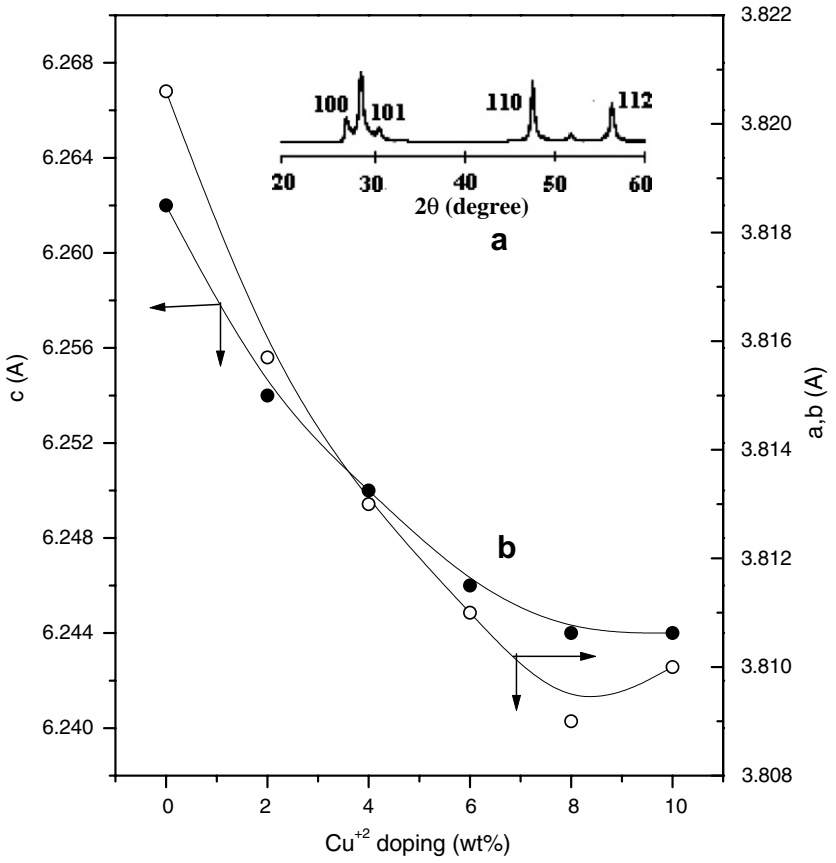

Fig. 2. XRD pattern of copper-doped ZnS particles (a) and cell constants against Cu^{2+} doping showing the lattice contraction and XRD spectra of ZnS (b). Cu^{2+} concentration 3% (mol).

formation in the PEG-process appears to be responsible to an increased solubility of Cu in ZnS particles due to the high surface reactivity of powders.

Fig. 3 shows the photoluminescence intensity of Cu-doped ZnS. From this figure, one can observe that 3 mol% Cu-doped ZnS provides the best emission efficiency which agrees with the data reported for the ZnS doped with other dopant ions [56].

Fig. 4 shows the emission luminescence spectra at excitation wavelength (λ_{exc}) of 400 nm of both ZnS and ZnS:Cu, respectively. The samples were found to be good absorbers of UV-visible radiation with emission features at 475 nm (ZnS) associated to the self-activated emission due to the defects in ZnS or the electronic transitions of the sulfur at the interface of ZnS grains [56]. The observed emission at 540 nm for the ZnS:Cu phosphor may be associated to the 3d level transitions of Cu^{2+} and a red shift in the emission wavelength in ZnS doped with Cu^{2+} is observed.

The synthesis of luminescent ZnS nanocrystals in PEG occurs by chemical reactions that result in the formation of stable nuclei and subsequent particle growth. The nucleating capability of PEG may be correlated with the interaction between the Zn^{2+} and the polyol, initiating the formation of the ZnS subcritical nuclei after condensation with thiourea [57].

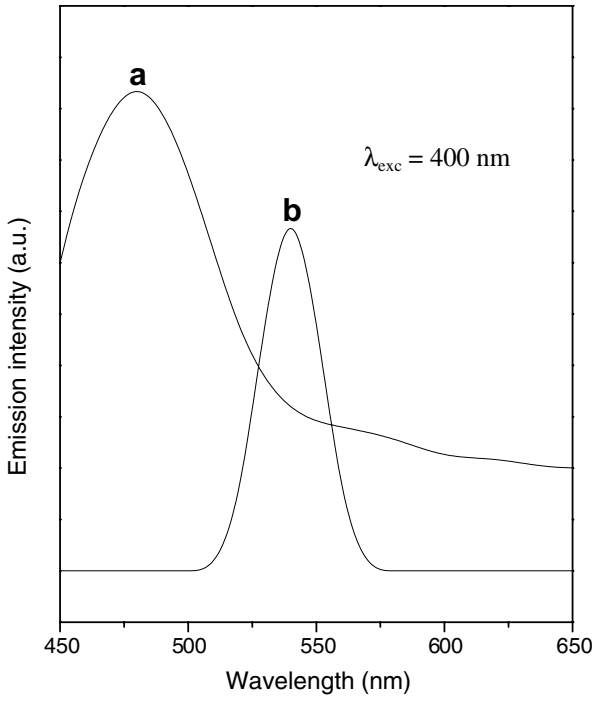

Fig. 4. Luminescence spectra of ZnS (a) and ZnS:Cu (b) at room temperature (27 °C).

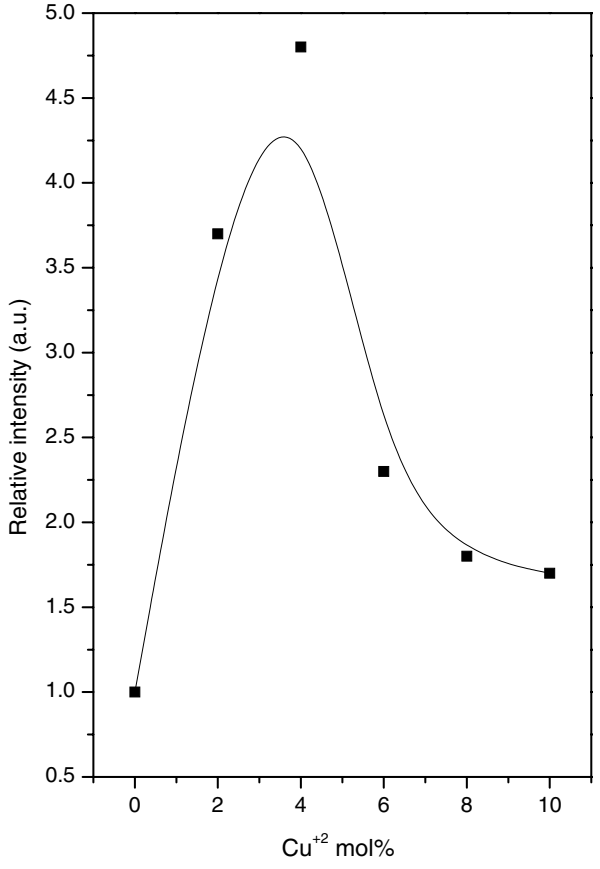

Fig. 3. Dependence of the peak intensity of the photoluminescence on the amount of Cu dopants in ZnS:Cu powder phosphors at room temperature (27 °C). The results of ZnS:Cu intensities are relative to the ZnS intensity.

As previously reported the PEG:Zn^{2+} complexes can be obtained by reacting zinc chloride and PEG where zinc remains fixed at the end of the polymer chain surrounded by oxygen atoms of the PEG (Scheme 2).

It is well known from FTIR studies that thiourea ligand coordinate through the sulfur atom with Zn^{2+} due to their zwitterionic form [58,59]. The organometallic ZnS precursor (PEG:Zn^{2+}:TU) produces S^{2-} anions by thermolysis and react rapidly with Zn^{2+} ions producing ZnS in the solution. In this sense, the NH_2 group of thiourea appears to be useful to the nucleation sites for the synthesis of ZnS nanocrystals. A possible mechanism explaining the ZnS synthesis from the polyol process can be represented by Scheme 2.

The analysis of the PEG:Zn^{2+} and PEG:Zn^{2+}:TU chelating processes during chemical reaction to form ZnS would be important to consider the frontier orbitals highest occupied molecular orbital (HOMO) and the lowest unoccupied molecular orbital) (LUMO) energies. In this case, the inverse dependence of stabilization energy on orbital energy difference will provide the dominant contribution.

An excellent ZnS precursor may be considered to be an organic compound that not only offer electrons to unoccupied d orbitals of a metallic ion to form a coordinate covalent bond, but also can accept the free electrons from the metal ion as well, by using their antibond orbital to form feedback bonds in turn.

It is well known from the quantum theory that soft molecules will be more reactive than hard molecules for the

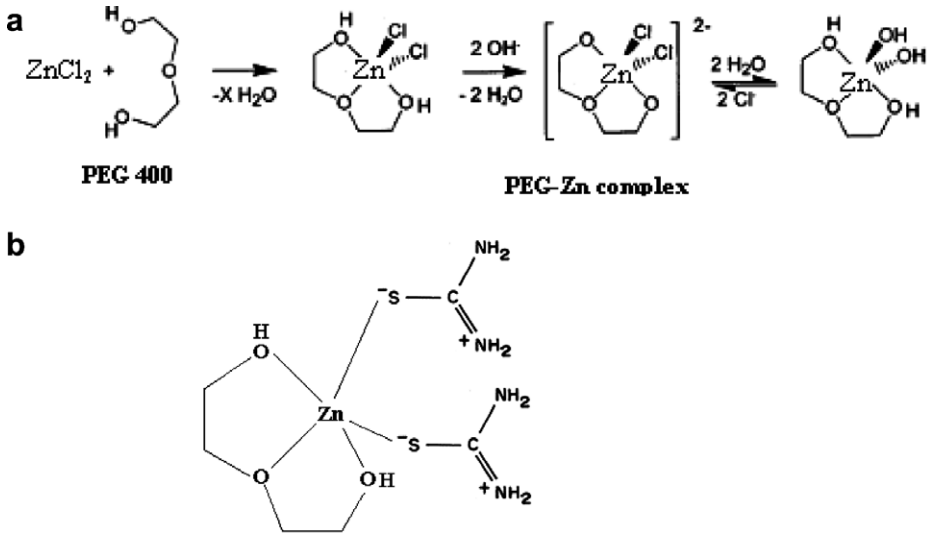

Scheme 2. Chemical reaction between PEG and $ZnCl_2$ for the synthesis of PEG:Zn^{2+} complex (a) and the PEG:Zn^{2+}:TU complex (b).

dissociation reactions [60,61]. A hard molecule has a large HOMO–LUMO gap and a soft molecule has a small HOMO–LUMO gap. A small HOMO–LUMO gap automatically means small excitation energies to the multiplets of excited states and the electron density changed more easily than a hard molecule

With the rapid advances in the field of nanotechnology during the last decade, many quantum dots have been produced through thermolysis of PEG:M (M = metal) complexes where the glycol is used as the reducing agent. This method is very attractive to produce the metal powders with a good control in size, monodispersity and shape [62,63].

The reaction pathway for the synthesis of ZnS nanocrystals involves initially the formation of the PEG:Zn^{2+} complex where the ether units in PEG is an active binding site to form the charge–transfer complex with the metallic ion. The HOMO–LUMO electronic density distribution in PEG:Zn^{2+} and PEG:Zn^{2+}:TU are plotted in Fig. 5. In the Zn^{2+} complex, all of d orbitals of the metal ion are occupied including the Zn $d_{x^2-y^2}$-O pπ orbital. Thus, the π contribution to covalence is canceled and the interaction and the covalent bonding interactions between the Zn 3d orbitals and the PEG orbitals become very small. In this case the only remaining covalent interactions come from Zn 4s, 4p orbitals (Fig. 5). In according to the transition state theory of chemical reactions, the reaction rate will increase as LUMO energy decreases, meaning the HOMO/LUMO energy difference will be smaller and electron transfer will be easily facilitated.

The accepted reaction mechanism between PEG:Zn^{2+}:TU involves the reactants approaching each other on parallel planes, with new bonds forming as a result of the overlap of π-electrons clouds (with the sulfur atom in thiourea as withdrawing electrons). Accordingly, the reaction depends on the interaction between the sulfur's highest occupied molecular orbital (HOMO) of TU and the lowest unoccupied molecular orbital (LUMO) of PEG:Zn^{2+} complex. The PEG:Zn^{2+}:TU complex has the smallest HOMO–LUMO gap (i.e. 1.21 eV) while PEG:Zn^{2+} (4.70 eV) has the highest energy gap. The HOMO electronic density distribution of TU clearly indicates the nucleophilic center of sulfur atom. The low value computed for the LUMO energy of PEG:Zn^{2+} complex implies that this molecule should possess a highest affinity to sulfur electron of thiourea (Fig. 5).

Despite its simplicity, the local ionization potential surrounding a molecule may be very useful in providing detailed information on the contributions of specific regions on the molecules to the chemical reactivity. An isosurface for which the LIP delineates by the gradation of the LIP regions in a molecule those are subject to electrophilic attack.

The LIP of the PEG:Zn^{2+} and the PEG:Zn^{2+}:TU species are displayed in Fig. 6. In Fig. 6a the highly ionization energy value of the PEG:Zn^{2+} indicates that the Zn is a highly reactive site with a strong electrophylic character. The large size and polarizability of thiourea leads to the sulfur atom ability to form stable polycoordinate and a strong tendency to form charge–transfer complex with PEG:Zn^{2+}. Analyses of the isopotential surface of both, PEG:Zn^{2+} and PEG:Zn^{2+}:TU complexes (Fig. 6) revealed that sulfur atom is an active site of the complex and the highly nucleophilic character of the TU relatively to PEG is evidenced.

Fig. 6 shows the local electron affinity at the backside of PEG:Zn^{2+} and PEG:Zn^{2+}:TU complexes. The gradation of the local ionization energy in the relevant areas of the molecular surfaces from deactivated PEG:Zn^{2+} complex through PEG:Zn^{2+}:TU complex are clearly seen. The position of attack of TU in PEG:Zn^{2+} complex can be seen clearly from the areas of most positive local electron affinity (i.e. those areas where accepting an electron is most favorable) at the backside of molecules. In this sense,

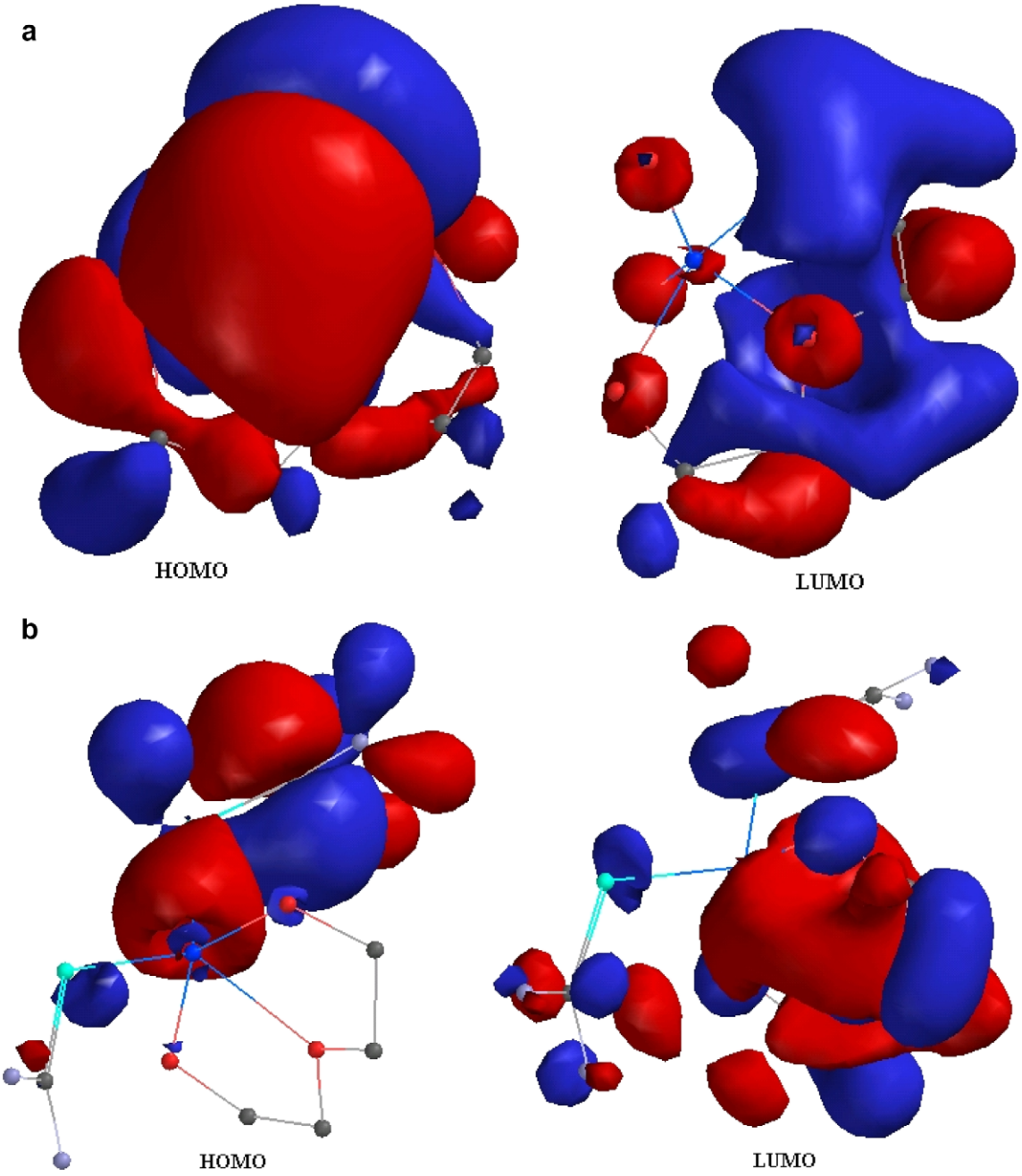

Fig. 5. Contour surfaces of frontier orbitals of the PEG:Zn^{2+} (a) and PEG:Zn^{2+}:TU complexes (b).

Fig. 6b suggests that there is at least a qualitative correlation between the local ionization energy on the molecular surface from the PEG:Zn^{2+}:TU and the reactivity of the molecule. From the Fig. 6b it is may be concluded that thiolate group in TU are stronger nucleophile than their oxygen equivalent in PEG:Zn^{2+} complex.

Zinc sulfide quantum dots have been the object of intensive studies in recent decades. However, in spite of the large number of investigations about the ZnS quantum dots synthesis the theoretical studies are extremely scarce and, as far as the authors are aware, no DFT–LDA investigations about this ceramic synthesis were reported till the moment. The agreement between the DFT–LDA and the experimental observations in this work suggests that the ZnS quantum dots can be investigated by this technique.

4. Conclusion

The local density functional theory (DFT) has emerged as an accurate alternative ab initio approach to quantum mechanical molecular studies with low computational cost. In recent years, the DFT methods has transformed in a competitive methodology relatively to the semi-empirical models. Importantly for experimental chemists, the results of DFT calculations can be communicated in the familiar terms of molecular orbital theory.

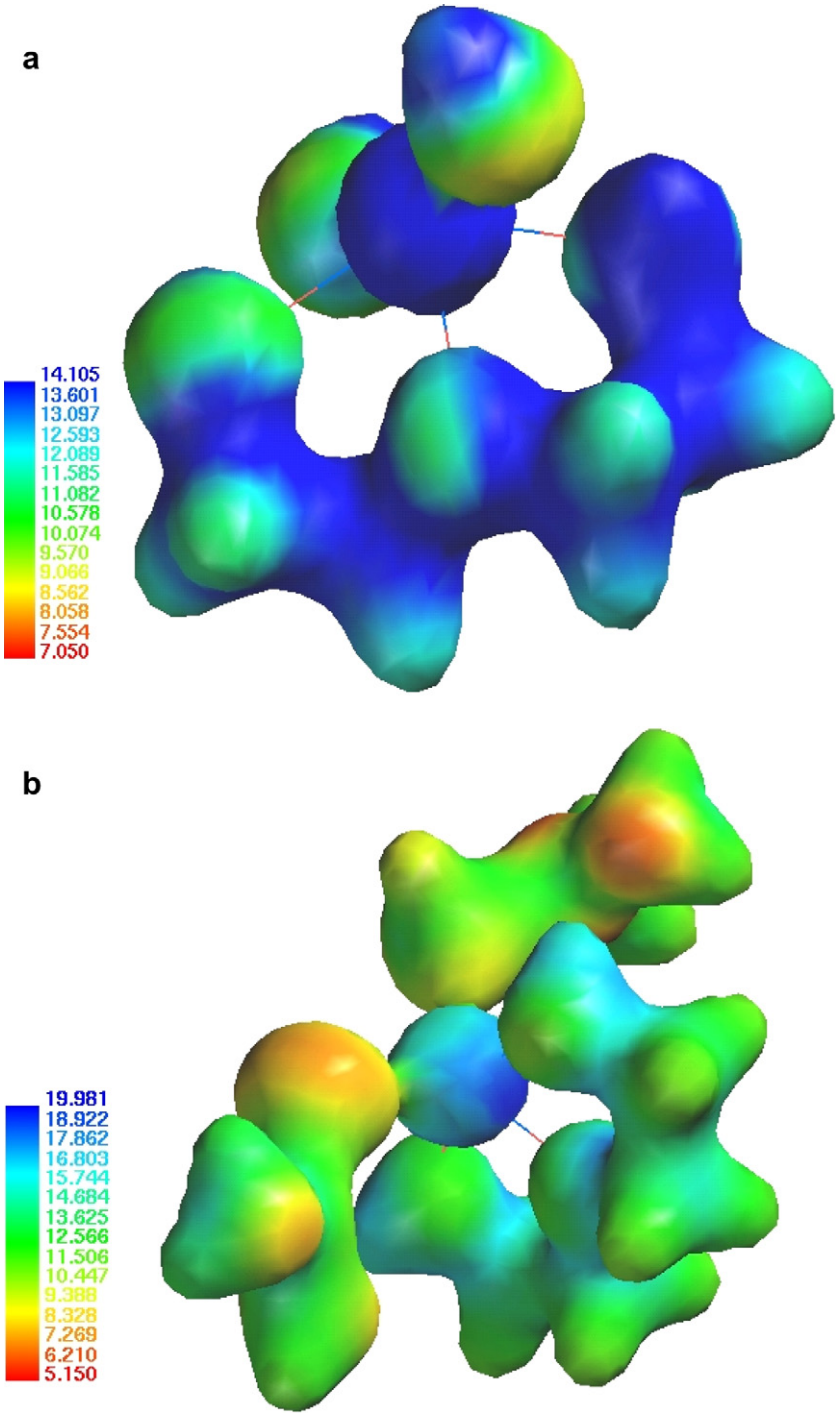

Fig. 6. Ionization potential mapped on the surface of the total electron density of the PEG:Zn^{2+} (a) and PEG:Zn^{2+}:TU (b) complex.

From the above studies, it has been established that the PEG-process may be used for the preparation of efficiently luminescent ZnS nanocrystals. The formation of ZnS particles in situ with wurtzite structure has been observed by XRD. The formation of homogeneous and not agglomerated powders indicates that PEG-process can be used for making luminescent ZnS powders with high purities and brightness. This method is economical and may be a promising chemical route for inorganic phosphors synthesis. The local properties of the PEG:Zn^{2+} and PEG:Zn^{2+}:TU complexes was calculated to describe the donor/acceptor character of regions of precursors. In this sense, frontier orbitals and LIP provide a more complete description of the intermolecular interactions between the precursors of the ZnS and some aspects of the chemical reactivity can be used in quantitative predictions of reactions rates and products.

Acknowledgment

The authors are grateful for the support of the CNPq.

References

[1] S. Luryi, J. Xu, A. Zaslawsky, Future Trends in Microelectronics: The Nanomillennium, Wiley-IEEE Press, New York, 2003.
[2] Y.T. Hase, T. Kano, E. Nakazawa, H. Yamamoto, Adv. Electron. Electron Phys. 79 (1990) 271.
[3] G. Blasse, B.C. Grabmaier, Luminescent Materials, Springer-Verlag, New York, 1994.
[4] A. Lempicki, J. Wojtowicz, C. Becher, Wide-Gap Luminescent Materials, Kluwer Academic Publishers, Boston, 1997.
[5] D. Pletcher, F.C. Walsh, Industrial Electrochemistry, Chapman & Hall, London, 1993.
[6] A. Ghis, R. Meyer, P. Rambaud, F. Levy, T. Leroux, IEEE Trans. Electron. Devices 38 (1991) 2320.
[7] S. Shionoya, W.M. Yen, Phosphor Handbook, Editor ISBN, New York, 1998.
[8] H. Bechtel, W. Czarnojan, M. Haase, W. Mayr, H. Nikol, Phillip. J. Res. 50 (1996) 433.
[9] S.S. Manoharan, S. Goyal, M.L. Rao, M.S. Nair, A. Pradhan, Mater. Res. Bull. 36 (2001) 1039.
[10] G. Laukaitis, S. Lindroos, S. Tamulevicius, M. Leskela, Appl. Surf. Sci. (2001) 1.
[11] M. Konishi, T. Isobe, M. Senna, J. Lumin. 93 (2001) 1.
[12] P. O'Brien, J. McAleese, J. Mater. Chem. 8 (1998) 2309.
[13] B. Elidrissi, M. Addou, M. Regragui, A. Bougrine, A. Kachouane, J.C. Bernède, Mater. Chem. Phys. 68 (2001) 175.
[14] P.J. Dean, A.D. Pitt, M.S. Skolnick, P.J. Wright, B. Cockayne, J. Crystal Growth 59 (301) (1982).
[15] M. Tonouchi, S. Young, M. Tarsuro, S. Hirosh, O. Masaki, J. Appl. Phys. 2 (1990) L2453.
[16] H.-Y. Lu, S.Y. Chu, J. Crystal Growth 265 (2004) 476.
[17] S.H. Yu, J. Yang, Y.T. Qian, M. Yoshimura, Chem. Phys. Lett. 361 (2002) 362.
[18] M. Konishi, T. Isobe, M. Senna, J. Lumin. 93 (2001) 1.
[19] P.Y. Silvert, K. Tekaia-Elhsissen, Solid State Ionics 82 (1995) 53.
[20] A.M. Derfus, W.C.W. Chan, S.N. Bhatia, Nano Lett. 4 (2004) 11.
[21] D.S. Wang, J.B. He, N. Rosenzweig, Z. Rosenzweig, Nano Lett. 4 (2004) 409.
[22] A.C.S. Samia, X. Chen, C. Burda, J. Am. Chem. Soc. 125 (2003) 15736.
[23] A.P. Alivisatos, K.P. Johnson, X. Peng, T.E. Wilson, C.P. Loweth, M.P. Bruchez, P.G. Schultz, Nature 382 (1996) 609.
[24] D. Wang, A. Rogach, F. Caruso, Nano Lett. 2 (2002) 857.
[25] A. Sukhanova, J. Devy, L. Venteo, H. Kaplan, M. Artemyev, V. Oleinikov, D. Klinov, M. Pluot, J.H.M. Cohen, I. Nabiev, Anal. Biochem. 324 (2004) 60.
[26] P. Alivisatos, Nat. Biotechnol. 22 (2004) 47.
[27] S. Kulmala, J. Suomi, Anal. Chim. Acta 500 (2003) 21.
[28] W.G. Becker, A.J. Bard, J. Phys. Chem. 87 (1983) 4888.
[29] J. Robertson, M.J. Powell, Appl. Phys. Lett. 44 (1984) 415.
[30] L.E. Brus, J. Phys. Chem. 90 (1986) 2555.
[31] R.N. Bharagava, D. Gallagher, Phys. Ver. Lett. 72 (1994) 416.
[32] I. Kandarakis, D. Cavouras, D. Nikopoulos, A. Anastasiou, N. Dimitropoulos, N. Kalivas, E. Ventouras, I. Kalatzis, C. Nomicos, G. Panayiotakis, Radiat. Meas. 39 (2005) 263.
[33] B. Elidrissi, M. Addou, M. Regragui, A. Bougrine, A. Kachouane, J.C. Bernède, Mater. Chem. Phys. 68 (2001) 175.
[34] P.J. Dean, A.D. Pitt, M.S. Skolnick, P.J. Wright, B. Cockayne, J. Crystal Growth 59 (301) (1982).
[35] M. Tonouchi, S. Young, M. Tarsuro, S. Hirosh, O. Masaki, J. Appl. Phys. 2 (1990) L2453.
[36] H.-Y. Lu, S.Y. Chu, J. Crystal Growth 265 (2004) 476.
[37] S.H. Yu, J. Yang, Y.T. Qian, M. Yoshimura, Chem. Phys. Lett. 361 (2002) 362.
[38] M. Konishi, T. Isobe, M. Senna, J. Lumin. 93 (2001) 1.
[39] P.Y. Silvert, K. Tekaia-Elhsissen, Solid State Ionics 82 (1995) 53.
[40] G.M. Chow, L.K. Kurihara, K.M. Kemner, P.E. Schoen, W.T. Elam, A. Ervin, S. Keller, Y.D. Zhang, J. Budnick, T. Ambrose, J. Mater. Res. 10 (1995) 1546.
[41] M.S. Hedge, D. Larcher, L. Dupont, B. Beaudoin, K. Tekaia-Elhsissen, J.M. Tarascon, Solid State Ionics 93 (1997) 33.
[42] S.B. Alves, A.A.A. de Queiroz, O.Z. Higa, Artif. Organs 27 (2003) 444.
[43] S.R. Gadre, A. Taspa, J. Mol. Graph. 12 (1994) 45.
[44] P. Hohenberg, W. Kohn, Phys. Rev. B 136 (1964) 864.
[45] W. Kohn, L.J. Sham, Phys. Rev. A 140 (1965).
[46] P.A.M. Dirac, Proc. Camb. Phil. Soc. 26 (1930) 376.
[47] S.H. Vosko, L. Wilk, M. Nusair, Can. J. Phys. 58 (1980) 1200.
[48] T.A. Halgren, J. Comput. Chem. 17 (1996) 490.
[49] P. Sjoberg, J.S. Murray, T. Brinck, P. Politzer, Can. J. Chem. 68 (1990) 1440.
[50] P. Politzer, J.S. Murray, M.C. Concha, Int. J. Quantum Chem. 88 (2002) 19.
[51] G. Náray-Szabó, G.G. Ferenczy, Chem. Rev. 95 (1995) 829.
[52] G.M.S. El-Bahy, B.A. El-Sayed, A.A. Shabana, Vib. Spectrosc. 31 (2003) 101.
[53] T. Kaliyappan, P. Kannan, Prog. Polym. Sci. 25 (2003) 343.
[54] S.M. Sze, Physics of Semiconductor Device, Wiley Interscience Publication, New York, 1981.
[55] A.D. Dinsmore, D.S. Hsu, S.B. Qadri, J.O. Cross, T.A. Kennedy, H.F. Gray, B.R. Ratna, J. Appl. Phys. 88 (2000) 4985.
[56] H.Y. Lu, S.Y. Chu, J. Cryst. Growth 265 (2004) 476–481.
[57] D. Caruntu, Y. Remond, N.H. Chou, M.J. Jun, G. Caruntu, J. He, G. Goloverda, C. O'Connor, V. Kolesnichenko, Inorg. Chem. 41 (2002) 6137.
[58] A. Yamaguchi, R.B. Penland, S. Mizushima, T.J. Lane, C. Curran, J.V. Quagliano, J. Am. Chem. Soc. 80 (1958) 527.
[59] R.A. Bailey, T.R. Peterson, Can. J. Chem. 45 (1967) 1137.
[60] P. Sjoberg, J.S. Murray, T. Brinck, P. Politzer, Can. J. Chem. 68 (1990) 1440.
[61] P. Politzer, J.S. Murray, M.C. Concha, Int. J. Quantum Chem. 88 (2002) 19.
[62] G. Náray-Szabó, G.G. Ferenczy, Chem. Rev. 95 (1995) 829.
[63] R. Harpeness, Z. Peng, X. Liu, V.G. Pol, Y. Koltypin, A. Gedanken, J. Coll. Interf. Sci. 287 (2005) 678.